

THE INFLUENCE OF AN AMBIENT MAGNETIC FIELD ON RELATIVISTIC COLLISIONLESS PLASMA SHOCKS

CHRISTIAN BUSK HEDEDAL AND KEN-ICHI NISHIKAWA

Niels Bohr Institute, Department of Astrophysics, Juliane Maries Vej 30, 2100 København Ø, Denmark; and National Space Science and Technology Center (NSSTC), Gamma-Ray Astrophysics Team, 320 Sparkman Drive, Huntsville, AL 35805;

Draft version March 11, 2018

ABSTRACT

Plasma outflows from gamma-ray bursts, supernovae, and relativistic jets, in general, interact with the surrounding medium through collisionless shocks. The microphysics of such shocks are still poorly understood, which, potentially, can introduce uncertainties in the interpretation of observations. It is now well established that the Weibel two-stream instability is capable of generating strong electromagnetic fields in the transition region between the jet and the ambient plasma. However, the parameter space of collisionless shocks is vast and still remains unexplored. In this Letter, we focus on how an ambient magnetic field affects the evolution of the electron Weibel instability and the associated shock. Using a particle-in-cell code, we have performed three-dimensional numerical experiments on such shocks. We compare simulations in which a jet is injected into an unmagnetized plasma with simulations in which the jet is injected into a plasma with an ambient magnetic field both parallel and perpendicular to the jet flow. We find that there exists a threshold of the magnetic field strength below which the Weibel two-stream instability dominates, and we note that the interstellar medium magnetic field strength lies well below this value. In the case of a strong magnetic field parallel to the jet, the Weibel instability is quenched. In the strong perpendicular case, ambient and jet electrons are strongly accelerated because of the charge separation between deflected jet electrons and less deflected jet ions. Also, the electromagnetic topologies become highly non-linear and complex with the appearance of anti-parallel field configurations.

Subject headings: acceleration of particles, gamma rays: bursts, shock waves, instabilities, magnetic fields, plasmas

1. INTRODUCTION

The collisionless plasma condition applies to many astrophysical scenarios, including, the outflow from gamma-ray bursts (GRBs), active galactic nuclei, and relativistic jets in general. The complexity of kinetic effects and instabilities makes it difficult to understand the nature of collisionless shocks. Only recently, the increase in available computational power has made it possible to investigate the full three-dimensional dynamics of collisionless shocks.

In the context of GRB afterglows, observations indicate that shock-compressed magnetic field from the interstellar medium (ISM) is several orders of magnitude too weak to match observations. Particle-in-cell (PIC) simulations have revealed that the Weibel two-stream instability is capable of generating the required electromagnetic field strength of the order of percents of equipartition value (Frederiksen et al. (2004); Kazimura et al. (1998); Medvedev & Loeb (1999); Nishikawa et al. (2003, 2005); Silva et al. (2003)). Furthermore, PIC simulations have shown that in situ non thermal particle acceleration takes place in the shock transition region (Hededal et al. 2004; Hoshino & Shimada 2002; Saito & Sakai 2003). Three-dimensional simulations using $\sim 10^7$ electron-positron pairs by Sakai and Matsuo (2004) showed how complex magnetic topologies are formed when injecting a mildly relativistic jet into a force-free magnetic field with both parallel and perpendicular components. With a two-dimensional analysis, Saito & Sakai (2003) found that an ambient parallel magnetic field can quench the two-stream instability in the weakly relativistic case. In this Letter, we use three-dimensional PIC experiments to investigate how the two-stream instability is affected by the presence of an

ambient magnetic field. Using up to $\sim 10^9$ particles and $125 \times 125 \times 1200$ grid zones, we investigate the development of complex magnetic topologies when injecting a fully relativistic jet (bulk Lorentz factor $\Gamma = 5$) into an ambient magnetized plasma. Using varying field strengths, we focus on the case of a transverse magnetic field and compare it with the case of a parallel magnetic field. The simulations are mainly concerned with the electron dynamics since processes involving the heavier ions evolve on much longer timescales.

2. THE NUMERICAL EXPERIMENTS

We use the PIC code described by Frederiksen et al. (2004). The code works from first principles and evolves the equation of motion for the particles together with Maxwell's equations. In the simulation experiments, we inject an electron-proton plasma (a jet) into an ambient plasma (the ISM) initially at rest (Fig. 1). The jet is moving with a relativistic velocity of $0.98c$ along the z -direction corresponding to Lorentz factor $\gamma_{jet} = 5$. The ion-to-electron mass ratio is set to $m_i/m_e = 20$. The jet plasma and the ambient plasma have the same density, n , and the corresponding electron plasma rest-frame frequency $\omega_{pe} \equiv [ne^2/(m_e\epsilon_0)] = 0.035\Delta_t^{-1}$ (e is the unit charge, ϵ_0 the vacuum permittivity, and Δ_t the simulation unit time). We choose this low value in order to properly resolve the microphysics. Initially, the interface between the ambient and the injected plasma is located at $z = 3\lambda_e$, where λ_e is the electron skin depth defined as $\lambda_e \equiv c/\omega_{pe} = 28.6\Delta_x$ (c is the speed of light, and Δ_x the grid size). The time step and grid size obey the Courant-Friedrichs-Lewy condition $\Delta_t = 0.5\Delta_x/c$. Both plasma populations are, in their respective rest frames, Maxwellian distributed with a thermal electron velocity $v_{th} \simeq 0.03c$. This temperature allow us to numerically resolve the plasma Debye length with approxi-

mately one grid length.

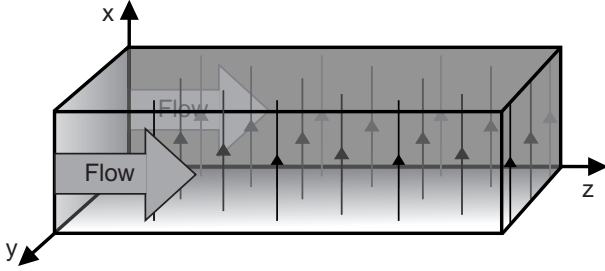


FIG. 1.— Schematic example of the simulation setup. Jet plasma is homogeneously and continuously injected in the z -direction throughout the x - y plane at $z = 0$. Inside, the box is populated by a plasma population, initially at rest. In this specific example, an ambient magnetic field is set up in the x -direction (perpendicular case).

We consider three different ambient magnetic configurations: no magnetic field, a magnetic field parallel to the flow, and a magnetic field perpendicular to the flow. The magnetic field is initially setup to be homogeneous and at rest in the ambient plasma. The experiments are carried out with 1 billion particles inside ($125 \times 125 \times 1200$) grid zones. In terms of electron skin depths, this corresponds to $(4.4, 4.4, 42)\lambda_e$. The boundary conditions are periodic in the direction transverse to the jet flow (x, y). In the parallel direction, jet particles are continuously injected at the leftmost boundary ($z = 0$). At the leftmost and rightmost z boundary, electromagnetic waves are absorbed, and we allow particles to escape in order to avoid unphysical feedback. The total energy throughout the simulations is conserved with an error less than 1%.

3. RESULTS

Initially, we run simulations with no ambient magnetic field and observe the growth of the Weibel two-stream instability also found in previous work (Frederiksen et al. (2004); Kazimura et al. (1998); Medvedev & Loeb (1999); Nishikawa et al. (2003, 2005); Silva et al. (2003)). The Weibel two-stream instability works when magnetic perturbations transverse to the flow collect streaming particles into current bundles that in turn amplify the magnetic perturbations. In the non linear stage, we observe how current filaments merge into increasingly larger patterns. The electromagnetic energy grows to $\epsilon_B \simeq 1\%$, where ϵ_B describes the amount of total injected kinetic energy that is converted to magnetic energy.

3.1. Parallel Magnetic Field

In the presence of a strong magnetic field component parallel to the flow, particles are not able to collect into bundles since transverse velocity components are deflected. We have performed five runs with parallel magnetic fields corresponding, respectively, to $\omega_{pe}/\omega_{ce} = 40, 20, 10, 5$, and 1 while keeping ω_{pe} constant; $\omega_{ce} = eB/(\gamma_{jet}m_e)$ is the jet electron gyrofrequency. The resulting field generation efficiency can be seen in Fig. 2 at $t = 21\omega_{pe}^{-1}$ where the jet front has reached $z = 23\lambda_e$. In the case of $\omega_{pe}/\omega_{ce} = 40$, the Weibel instability overcomes the parallel field, and although initially slightly suppressed, it eventually evolves as in the case of no ambient magnetic field. Increasing the magnetic field to $\omega_{pe}/\omega_{ce} = 1$ effectively suppresses the instability. Thus, for an ISM strength magnetic field ($\omega_{pe}/\omega_{ce} \simeq 1500$) parallel to the plasma flow, the

Weibel two-stream instability will evolve unhindered, and the generated field will exceed the ISM field. We find from the simulations that it would take a milligauss strength parallel magnetic field to effectively quench the instability for a $\gamma = 5$ jet expanding in an environment with density like the ISM.

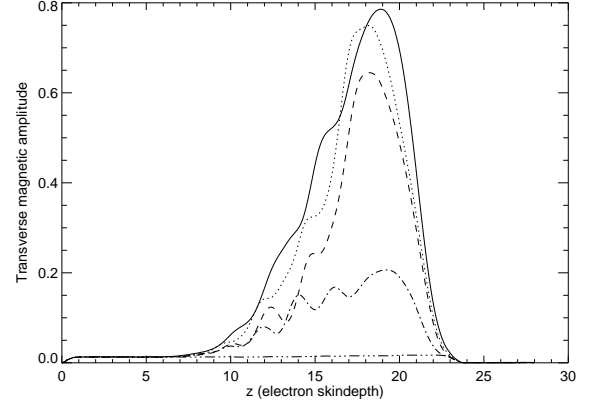


FIG. 2.— Growth of the Weibel two-stream instability for different strengths of the parallel ambient magnetic field at time $t = 21\omega_{pe}^{-1}$. Here we measure the effectiveness of the field generation as the average transverse magnetic field amplitude as a function of z . The solid line corresponds to $\omega_{pe}/\omega_{ce} = 40$, the dotted line to 20, the dashed line to 10, the dot-dashed line to 5, and the triple-dot-dashed line to 1. The case of no ambient magnetic field is very similar to that of $\omega_{pe}/\omega_{ce} = 40$. The magnetic amplitude is in arbitrary units

The left panel of Fig. 3 show the resulting electron momentum distribution function for different values of ω_{pe}/ω_{ce} at $t = 30\omega_{pe}^{-1}$. Since the presence of a strong parallel magnetic field suppresses the generation of a transverse magnetic field, there exists no mechanism that can heat the electrons and transfer momentum between the two electron populations. Thus the jet plasma propagates unperturbed. Where there is no parallel magnetic field or only a weak magnetic field ($\omega_{pe}/\omega_{ce} = 1500$), we observe how the jet and ambient plasma is heated and how momentum is transferred between the two populations.

3.2. Perpendicular Magnetic Field

We have performed experiments with an ambient magnetic field perpendicular to the jet flow (Fig. 1) with field strengths corresponding to $\omega_{pe}/\omega_{ce} = 1500, 40, 20$ and 5. By including the displacement current, one can derive the relativistic Alfvén speed $v_A^{-2} = c^{-2} + (v_A^{non-rel.})^{-2} \simeq c/[1 + (\omega_{pe}/\omega_{ce})^2(m_i/m_e)\gamma_{jet}^2]^{1/2}$, where $v_A^{non-rel.} = B/[\mu_0 n(m_i + m_e)]^{1/2}$ is the non-relativistic counterpart. From this we calculate the corresponding relativistic Alfvén Mach numbers $\gamma_{jet}v_{jet}/v_A = 6572, 175, 88$, and 22.

Again, the $\omega_{pe}/\omega_{ce} = 1500$ run has been chosen because it resembles the typical density and microgauss magnetic field strength of the ISM. We find that the magnetic field generated by the two-stream instability dominates the ambient magnetic field, and the result resembles that of no ambient magnetic field. Furthermore, as expected in both the parallel and perpendicular cases, the electron momentum distributions (Fig. 3) are very similar, except for a weak merging between the ambient and jet electrons in the perpendicular case.

In the run with $\omega_{pe}/\omega_{ce} = 20$, the result differs substantially from the previous cases. With reference to Fig. 4, we de-

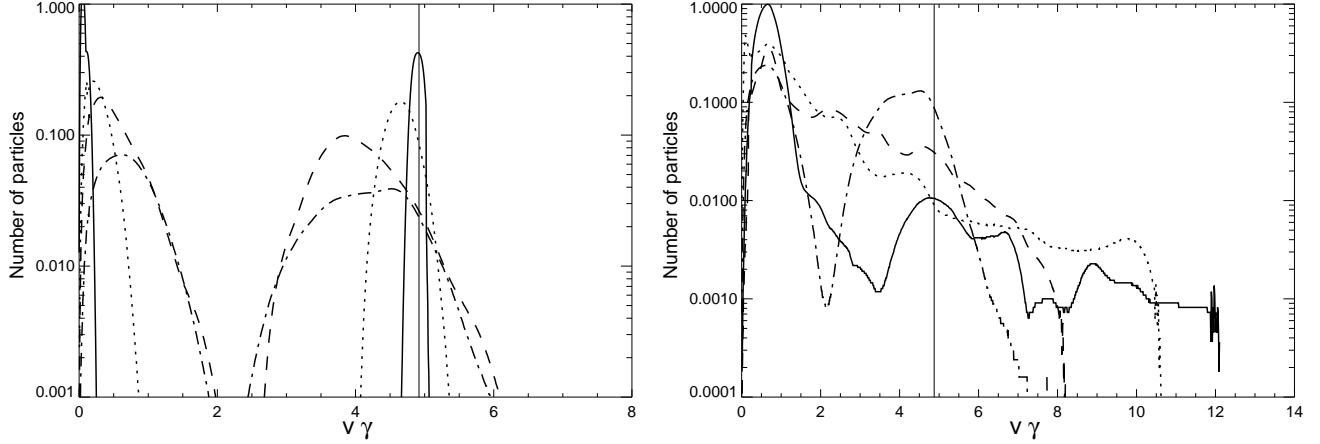


FIG. 3.— Normalized electron momentum distribution functions at time $30\omega_{pe}^{-1}$. The left panel is for runs with an ambient magnetic field parallel to the injected plasma with $\omega_{pe}/\omega_{ce} = 1$ (solid line), 20 (dotted line), 40 (dashed line), and 1500 (dot-dashed line). The right panel is for runs in which the initial magnetic field is perpendicular to the inflow and $\omega_{pe}/\omega_{ce} = 5$ (solid line), 20 (dotted line), 40 (dashed line) and 1500 (dot-dashed line). The vertical line shows the injected momentum $\gamma = 5$. The distribution functions are for electrons with $z > 15\lambda_e$.

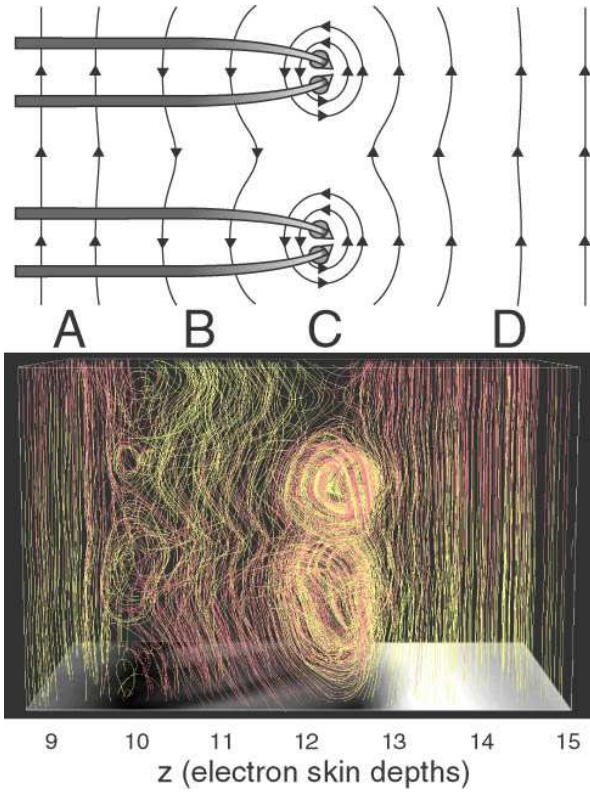


FIG. 4.— Snapshot at $t = 16\omega_{pe}^{-1}$ of the highly complicated magnetic field topology when a jet is injected into a plasma with an ambient magnetic field transverse to the jet flow. The bottom panel shows magnetic field lines in a subsection of the computational box (from $z = 9\lambda_e$ to $z = 15\lambda_e$). The top panel shows a schematic explanation in the x - z plane: Jet electrons are bent by the ambient magnetic field (region A). Due to the Weibel instability, the electrons bundle into current beams (region C) that in turn reverse the field topology (region B). This will eventually bend the jet beam in the opposite direction. [See the electronic edition of the Journal for a color version of this figure.]

The magnetic field is piled up behind the jet front, and the enhanced magnetic fields bend jet electron trajectories sharply. This has two implications. First, the ions, being more massive, will penetrate deeper than the deflected electrons. This creates a charge separation near the jet head that effectively accelerates both ambient and injected electrons behind the ion jet front as shown in Fig. 5. Second, the deflected electrons eventually become subject to the Weibel two-stream instability. This forms electron current channels at some angle to the initial direction of injection, as shown in the upper panel of Fig. 4. Around these current channels, magnetic loops are induced (Fig. 4, region C). Magnetic islands are formed and the ambient magnetic field is reversed behind the loops (region B). In this region, we find acceleration of electrons in the x -direction. The activity in this region has similarities to reconnection, but it is beyond the scope of this Letter to investigate this topic.

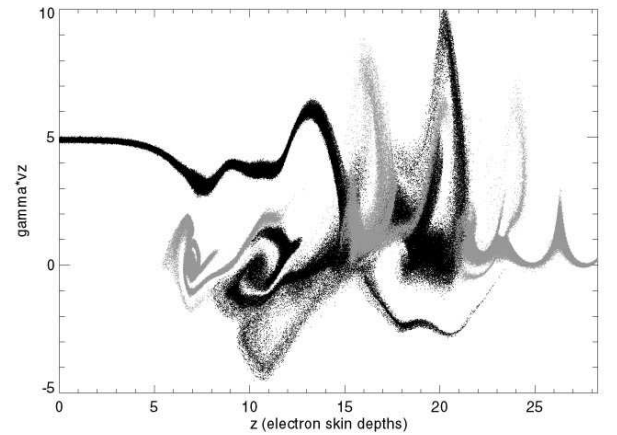


FIG. 5.— Electrons $v_z\gamma$ plotted against their position in the shock at time equal $30\omega_{pe}^{-1}$ for the run with an ambient magnetic field transverse to the jet flow corresponding to $\omega_{pe}/\omega_{ce} = 20$. The jet electrons (black dots) are injected at $z = 0$ with $\gamma = 5$. The ambient electrons (gray dots) are initially at rest but are strongly accelerated by the jet.

scribe the different stages of the evolution: Initially, the injected particles are deflected by the ambient magnetic field.

In other regions, the ambient magnetic field is strongly compressed, and this amplifies the field strength up to 5 times the initial value. As a result, parts of the jet electrons are actually reversed in their direction. This can be seen from Fig. 5, which shows a phase-space plot of both ambient and jet electrons at $t = 30\omega_{pe}^{-1}$. We see several interesting features here. In the region $z = (15-21)\lambda_e$, we observe how ambient electrons are swept up by the jet. Behind the jet front, both ambient and jet electrons are strongly accelerated since the jet ions, being heavier, take a straighter path than the jet electrons, and this creates a strong charge separation. The excess of positive charge in the very front of the jet head is very persistent and hard to shield since the jet ions are moving close to the speed of light. Thus, there is a continuous transfer of z -momentum from the jet ions to the electrons. In the case of the perpendicular ambient field, more violent processes take place than in the case of the parallel field, which can be seen in Fig. 3 (*right panel*). Here we see that mixing of the two plasma populations is much more effective for the perpendicular case. However, the spectrum of the electrons' momentum is highly nonthermal, with strong acceleration of both jet and ambient electrons. The cutoff in electron acceleration depends on the magnetic field strength. The maxima ($\gamma v_{\parallel} \approx 10$) at $z = 20\lambda_e$ in Fig 5 corresponds to the cutoff shown by the dotted line in the right panel in Fig. 3. It should be noted that the current channels that are caused by the bent jet electron trajectories in the early time, as shown in Fig. 4, are also seen in Fig. 5. The first current channels have moved to around $z = 20\lambda_e$. At $z = 15\lambda_e$, a second current channel is created by the deflected jet electrons. This periodic phenomenon involves the ions in a highly nonlinear process but is beyond the scope of this Letter and will be explained in a subsequent paper.

4. CONCLUSIONS

Using a three-dimensional relativistic particle-in-cell code, we have investigated how an ambient magnetic field affects the dynamics of a relativistic jet in the collisionless shock region. We have examined how the different ambient magnetic topology and strength affect the growth of the electron Weibel two-stream instability and the associated electron acceleration. This instability is an important mechanism in collisionless shocks. It facilitates momentum transfer between colliding plasma populations (Frederiksen et al. 2004; Kazimura et al. 1998; Medvedev & Loeb 1999; Nishikawa et al. 2003, 2005;

Silva et al. 2003) and can accelerate electrons to nonthermal distributions (Hededal et al. 2004; Hoshino & Shimada 2002; Saito & Sakai 2003). Collisionless shocks are found in the interface between relativistic outflows (e.g., from gamma-ray bursts and active galactic nuclei) and the surrounding medium (e.g., the ISM).

We find substantial differences between the cases of ambient magnetic fields transverse and parallel to the jet flow. However, common for both cases is that it takes an ambient magnetic field strength much stronger than the strength of the magnetic field typically found in the ISM to effectively suppress the Weibel two-stream instability. In the case of a parallel magnetic field, ω_{pe}/ω_{ce} must be smaller than 5 to effectively suppress the instability. This result is in good agreement with two-dimensional simulations by Saito & Sakai (2003), and thus this limit seems independent of γ_{jet} . For a typical ISM density of $10^6 m^{-3}$, this corresponds to a milligauss magnetic field. We emphasize the importance of ω_{pe}/ω_{ce} as an important parameter for collisionless shocks, as was also pointed out by Shimada & Hoshino (2004).

In the case of perpendicular injection, the dynamics are different from the parallel injection. Here, the electrons are deflected by the magnetic field, and this creates a charge separation from the less deflected ions. The charge separation drags the ambient and jet electrons, and consequently they are strongly accelerated along the z -direction. Furthermore, due to the Weibel instability, current channels are generated around the ambient magnetic field, which is curled and locally reversed.

These simulations provide insights into the complex dynamics of relativistic jets. Further investigations are required to understand the detailed physics involved. Larger simulations (above 10^9 particles) with longer boxes are needed to cover the instability domain of the ions, to investigate the full evolution of the complicated dynamics, and to resolve the whole shock ramp.

This research (K.-I.N.) is partially supported by the National Science Foundation awards ATM 9730230, ATM-9870072, ATM-0100997, and INT-9981508 and (C.B.H.) by a grant from the University of Copenhagen. One of the authors C.B.H. would like to thank Dr. G. J. Fishman for his support and hospitality during a stay at the NSSTC - Huntsville Alabama, USA and Dr. Å. Nordlund for his help and guidance.

REFERENCES

- Frederiksen, J. T., Hededal, C. B., Haugbølle, T., & Nordlund, Å. 2004, ApJ, 608, L13
- Hededal, C. B., Frederiksen, J. T., Haugbølle, T., & Nordlund, Å. 2004, ApJ, 617, L107
- Hoshino, M., & Shimada, N. 2002, ApJ, 572, 880
- Kazimura, Y., Sakai, J. I., Neubert, T., and Bulanov, S. V. 1998, ApJ, 498, L183
- Medvedev, M. V., & Loeb, A. 1999, ApJ, 526, 697
- Nishikawa, K.-I.; Hardee, P.; Richardson, G.; Preece, R.; Sol, H.; Fishman, G. J. 2003, ApJ, 595, 555
- Nishikawa, K.-I.; Hardee, P.; Richardson, G.; Preece, R.; Sol, H.; Fishman, G. J. 2005, ApJ, 622, 927
- Sakai, J.-I. and Matsuo, A. 2004, Phys. Plasmas, 11, 3251
- Saito, S., & Sakai, J.I. 2003, Phys. Plasma, 11, 859
- Shimada, N., & Hoshino, M. 2004, Phys. Plasmas, 11, 1840
- Silva, L. O. and Fonseca, R. A. and Tonge, J. W. and Dawson, J. M. and Mori, W. B. and Medvedev, M. V. 2003, ApJ, 596, L121